

---

# Three-Dimensional Functional Images of Myocardial Oxygen Consumption from Positron Tomography

Tom R. Miller, Jerold W. Wallis, Edward M. Geltman, and Steven R. Bergmann

*The Edward Mallinckrodt Institute of Radiology, St. Louis, Missouri and Cardiovascular Division, Department of Internal Medicine, Washington University School of Medicine, St. Louis, Missouri*

---

Images from positron emission tomography (PET) are usually presented as transaxial slices portraying tissue radioactivity. Studies can be difficult to interpret from transaxial images, and the temporal changes in tissue tracer concentrations which permit quantitative determinations of metabolism and perfusion are not displayed. We have developed a method to give quantitatively accurate three-dimensional images of myocardial oxygen consumption from serial images of the myocardial washout of carbon-11-acetate. Following i.v. bolus injection, data are collected for 20-30 min. The time-activity curves for each pixel in the transaxial slices are fit to a monoexponential function to determine the washout rate, which is directly related to the rate of myocardial oxygen utilization. Thus, functional images of myocardial oxygen consumption are produced for all seven slices of PET data. A previously developed method is then used to generate realistic and quantitatively accurate three-dimensional images.

**J Nucl Med 1990; 31:2064-2068**

---

**P**ositron emission tomography (PET) is an intrinsically quantitative technique, which permits the reconstruction of the distribution of positron emitting radio-nuclides within the body. Typically, reconstructed data are presented as transaxial images portraying tissue radioactivity, usually expressed as counts/pixel (picture element). Display of cardiac PET data in this manner limits full interpretation of such studies in two ways. First, viewing in the coordinate system of the body rather than in the long- and short-axis coordinates of the heart impedes diagnosis of abnormalities, especially in the inferoposterior myocardium which is not well visualized in the transverse plane (1). More important, transverse images as currently displayed represent only the count-based sum of radioactivity per pixel per unit time. The temporal information that is typically ac-

quired in dynamic PET studies and which permits calculation of absolute rates of metabolism or perfusion when coupled with a mathematical model is not displayed.

We (2-6) and others (7-10) have developed and validated a method for estimation of myocardial oxygen consumption ( $M\dot{V}O_2$ ) noninvasively by applying a physiologically and mathematically appropriate model to dynamic PET data. This approach uses the tissue time-activity information reconstructed from dynamic data collected in sequential frames to enable assessment of time-activity relationships. This information is used to calculate oxidative metabolism in absolute terms. Currently, to estimate regional  $M\dot{V}O_2$ , manually-drawn regions of interest are first placed on transverse, count-based images, and then the time-activity data obtained from the dynamic acquisitions are input into the mathematical model. While estimates of metabolism are computed for selected large anatomic regions, it has not been possible to display this physiologically important quantity for visual analysis.

Carbon-11-acetate ( $^{11}\text{C}$ -acetate) can be used for estimation of myocardial oxygen consumption (2-10). Acetate is avidly extracted by the myocardium and is oxidized exclusively in the mitochondria. Since mitochondrial oxidation is tightly coupled to oxidative phosphorylation, and since other pathways for metabolism of acetate by the heart are modest, the oxidation of  $^{11}\text{C}$ -acetate to  $^{11}\text{CO}_2$  and the subsequent clearance of  $^{11}\text{CO}_2$  from the heart provides an index of myocardial oxygen consumption. We have validated the relationship between the clearance of  $^{11}\text{C}$  radioactivity from the myocardium and myocardial oxygen consumption measured directly over a wide range of flow and metabolic conditions. In addition, we recently demonstrated that the relationship between  $^{11}\text{C}$  clearance and  $M\dot{V}O_2$  is not influenced by the pattern of substrate utilization (4).

To facilitate interpretation of PET studies of myocardial oxygen consumption and to address the deficiencies in display of PET studies described above, we have developed a method to represent cardiac PET data

---

Received Feb. 12, 1990; revision accepted Jun. 17, 1990.  
For reprints contact: Tom R. Miller, MD, PhD, The Edward Mallinckrodt Institute of Radiology, 510 S. Kingshighway Blvd., St. Louis, MO 63110.

in a more useful form as functional images of myocardial oxygen metabolism rather than as images of tissue radioactivity (11). We have employed a method previously developed in our laboratory for three-dimensional reconstruction of the heart from transverse PET data (12). This technique is combined with our mathematical approach for estimation of myocardial metabolism to enable display of myocardial metabolism as functional, three-dimensional images.

## METHODS

### Estimation of Oxidative Metabolism

Subjects were studied after informed written consent was obtained. All protocols were approved by our Institutional Review Board. A cross-section of routine studies were randomly selected from examinations performed as part of other research protocols at our institution. No studies were excluded for technical reasons. Five studies were transformed into functional images and four were from patients with acute myocardial infarction who were studied within 2-3 days of admission to the coronary care unit (three inferior, one anterior). Infarction was documented by analysis of plasma creatine kinase activity and by the presence of Q-waves on the electrocardiogram. One study was from a normal subject. Additional studies were not analyzed because of the excellent visual and quantitative results obtained in this initial group.

To estimate myocardial oxygen consumption, a bolus of  $^{11}\text{C}$ -acetate (0.35–0.4 mCi/kg) was administered intravenously via an antecubital vein. Data were collected in list mode for 20-30 min and reconstructed into serial 60-120-sec frames. The rate of myocardial oxygen utilization was determined by monoexponential fitting of the clearance of radiolabeled acetate beginning at 2-3 min after injection when blood-pool activity was negligible. The rate constant of  $^{11}\text{C}$  clearance after correction for radioactive decay was used to determine  $\text{M}\dot{\text{V}}\text{O}_2$  in units of  $\mu\text{mole/g/min}$  with use of a regression equation relating the two quantities that was derived from experimental studies in animals (3,4,6). This equation was obtained in 33 direct comparisons over a wide range of flow and metabolic conditions. Spillover and partial volume corrections were not employed since we have previously demonstrated that these corrections do not markedly influence the estimate of the turnover rate constant (3,5).

### Tomograph

Data were acquired with use of SuperPETT I, a PET tomograph employing time-of-flight. Seven transaxial slices were collected with a slice thickness of 1.14 cm and slice spacing of 1.5 cm. Images were reconstructed from list-mode data with a confidence-weighted algorithm, giving an effective resolution of 1.35 cm full width at half-maximum (FWHM). Transaxial slices were collected in a matrix size of  $128 \times 128$  pixels giving pixel dimensions of 3.5 mm  $\times$  3.5 mm. All data were corrected for attenuation with use of a scan obtained with an external ring of germanium-68/gallium-68.

### Digital Filtering

Since the goal of the present work is voxel-by-voxel determination of oxygen consumption, it was necessary to smooth the images to compensate for the relatively poor signal-to-

noise ratio of the data in the individual voxels. This step was not required in the earlier work (3-6), since  $\text{M}\dot{\text{V}}\text{O}_2$  was determined only in large myocardial regions typically consisting of 10-100 voxels encompassing 1-10  $\text{cm}^3$ . A low-pass digital filter was employed with a cutoff frequency of 0.3 cycles/cm (0.1 cycles/pixel). This cutoff frequency corresponds to the half-maximum frequency of the reconstruction filter used in the image generation—1.35 cm FWHM resolution is equivalent to 0.33 cycles/cm half width at half maximum for a Gaussian point-spread function (13). Filtering was implemented in the spatial domain with use of a finite-impulse-response digital filter following methods previously developed in our laboratory (14). The size of the two-dimensional convolution mask was  $15 \times 15$  pixels. To speed the calculations, processing was performed only in manually-drawn  $64 \times 64$  pixel regions completely encompassing the heart.

### Generation of Functional Images

After smoothing of the transaxial slices, the time-activity curves of each voxel were fit to a monoexponential function by the method of least squares for the 10-20 sequential time frames.  $\text{M}\dot{\text{V}}\text{O}_2$  was determined from the rate constant of exponential clearance for each time-activity curve, and the values were used to produce seven functional images showing  $\text{M}\dot{\text{V}}\text{O}_2$  for every voxel in each of the transaxial slices in the original data. The images are displayed within large, manually defined regions encompassing the entire epicardial border. The mean values of  $\text{M}\dot{\text{V}}\text{O}_2$  in 20 regions in mid- and low-ventricular slices of the functional images were compared to the values determined in the same subjects using the previously validated approach employing fitting of the regional time-activity curves from the unfiltered images (6). Six regions were drawn in areas of documented infarction while 14 regions were in normal myocardial segments. These regions encompassed 8-10 voxels with a volume of  $\sim 1 \text{ cm}^3$ . One transaxial slice was selected in each study that included the mid portion of the infarcted area or the normal zone. Inspection of the transaxial and three-dimensional images indicates that the selected regions are representative of the quantitative results that would be obtained in other myocardial segments. The analysis was performed on a minicomputer (MicroVAX II, Digital Equipment Corp., Maynard, MA). The total computation time required to filter the images and fit the 29,000 ( $64 \times 64 \times 7$ ) time-activity curves was  $\sim 3$  min.

### Three-dimensional Images of Oxygen Consumption

Three-dimensional images of  $\text{M}\dot{\text{V}}\text{O}_2$  were obtained from the transaxial functional images employing a method we developed and previously described in detail (12). First, the seven transaxial slices were trilinearly interpolated so that the voxel dimensions were equal. Then, the center of the left ventricle was specified by inspection of the cube of image data, and the angle of rotation of the heart was determined interactively. Next, the cubic data were rotated so the long axis of the heart was positioned vertically in the computer memory, giving the conventional short- and long-axis slice images. A radical search was then performed in three dimensions to find the voxel with greatest intensity along each ray. Finally, polar (bull's-eye), cylindrical, and surface displays were created from the three-dimensional map of greatest circumferential activity. Images computed at 32 angles around

the heart can be viewed in cine mode creating a display of the heart rotating about its long axis. Infrequent errors in positioning of the ventricular center and rotation angles can be identified readily by noting a wobbling motion of the ventricle during rotation and by asymmetry in activity in the periphery of the polar display caused by these errors. Eight minutes of computation time was required on a MicroVAX II to produce the three-dimensional images from the transaxial functional images.

## RESULTS

### Image Display

The upper images of Figure 1 show selected time frames from an unprocessed, count-based reconstruction at the mid-ventricular level obtained after administration of  $^{11}\text{C}$ -acetate in a patient with inferior wall myocardial infarction. The lower images show the same time frames following low-pass digital filtering. The functional images of  $\dot{M}\dot{V}\text{O}_2$  for selected transaxial slices are shown in Figure 2 for a normal subject and for the patient with inferior infarction.

The three-dimensional displays of the normal subject and the abnormal subject with inferior infarction are shown in Figures 3 and 4, respectively. In each case, the upper left image is the polar, bull's-eye display reflecting regional  $\dot{M}\dot{V}\text{O}_2$  viewed from the left-ventricular apex. Note the reduced oxygen utilization rate in the infarcted area in Figure 4 and the uniform distribution in the normal subject. The lower left image is a side view of the ventricle, the cylindrical display, that is analogous to the Mercator projection used in cartography. The two images on the right represent surface displays of myocardial  $\dot{M}\dot{V}\text{O}_2$  with the left ventricle oriented vertically. In the bottom image in Figure 4, the area of reduced oxygen utilization is suppressed, permitting viewing of the normal far wall of the ventricle. The surface images are generated at 32 angles around the heart, leading to a rotating cine display. Values of  $\dot{M}\dot{V}\text{O}_2$  ( $\mu\text{mol/g/min}$ ) are depicted in the bars on the sides of the figures.

### Quantitative Data

The mean values of  $\dot{M}\dot{V}\text{O}_2$  for the 20 regions in the five subjects are shown in Figure 5. The values determined with use of the previously validated method are shown on the abscissa while the results obtained from the functional images are presented on the ordinate.

## DISCUSSION

Estimates of myocardial oxygen consumption and its response to physical or pharmacologic stress (i.e., the metabolic reserve) are central to the diagnosis of a variety of cardiac disorders and their response to therapy. Positron emission tomography using  $^{11}\text{C}$ -acetate can provide sequential, noninvasive estimation of myocardial oxygen consumption in absolute terms. In pre-

vious work from our laboratory, we demonstrated the ability to quantify oxygen consumption and its reserve in human subjects from transverse count-based PET data (5-6). In that work,  $\dot{M}\dot{V}\text{O}_2$  was obtained in relatively large regions of myocardium corresponding to septal, anterior, lateral, and posterior myocardial regions. The new three-dimensional functional displays described here permit assessment of the inferoposterior wall, which is difficult to perceive in transverse reconstructions (1) (Figs. 1, 2, and 4), and a cine display is produced that permits viewing of the myocardium from all angles. In contrast to pure count-based reconstructions, these functional displays preserve the important time-based kinetic information. These images provide a visual counterpart to the numerical information derived previously only for selected anatomical regions. The quantitative accuracy of the functional images was verified by comparison to the previously validated technique employing  $1\text{ cm}^3$  regions (Fig. 5).

These displays facilitate perception of regional abnormalities in oxygen utilization. Since the entire left ventricular myocardium is visualized, failure to detect abnormal areas of myocardium through arbitrary assignment of regions is reduced, and the overall perception of the distribution of oxygen utilization is enhanced. Direct three-dimensional comparison with other tomographic measures of myocardial function and metabolism, e.g., with fluorine-18-fluorodeoxyglucose or gated blood-pool imaging (11-12), is now possible.

Studies in humans done at our institution (5-6) and elsewhere (7) have demonstrated that clearance of radioactivity from the myocardium at rest is monoexponential. Work from experimental animal studies from our institution (2-4) as well as from other laboratories (8,10) have demonstrated that clearance of radioactivity from the hearts of experimental animals is biexponential. However, the slow phase is very long in comparison to the rapid phase in animals and human subjects studied at rest, and the rapid phase correlates closely with invasive measurements in animals of  $\dot{M}\dot{V}\text{O}_2$ . Thus, we and others agree that use of a monoexponential fit is appropriate to determine myocardial oxygen utilization (5-10).

### Technical Considerations

Low-pass digital filtering employed before determination of  $\dot{M}\dot{V}\text{O}_2$  could lead to failure to detect small abnormalities through excessive smoothing of the images. This is not likely to occur in this case, however, since the cutoff frequency of the digital filter is the same as the FWHM used in reconstruction of the transaxial slices. Thus, the spatial resolution is limited by the characteristics of the positron tomograph and the reconstruction process, not by the additional filtering used here. Filtering could also lead to contamination of myocardial counts by residual activity in the cardiac

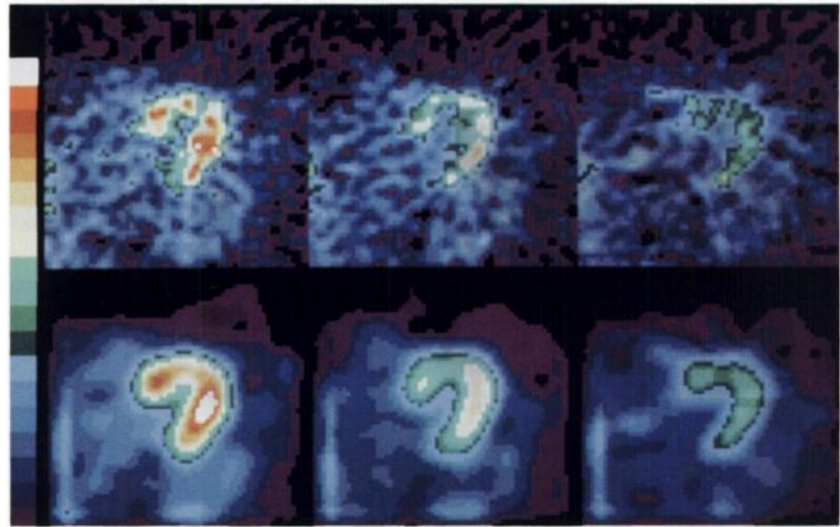


**FIGURE 1**  
Transaxial images at the mid-ventricular level of 1 min duration each are shown at 4, 7, and 10 min after injection of  $^{11}\text{C}$ -acetate in a patient with inferior wall myocardial infarction. Unprocessed reconstructions are shown on the top row while the same images are shown on the bottom row after low-pass digital filtering.

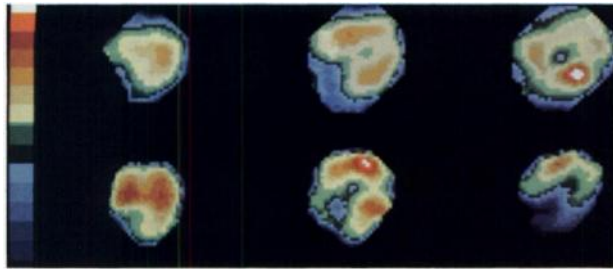


**FIGURE 2**  
Functional images of  $\dot{M}\text{V}\text{O}_2$  are shown for selected transaxial slices for a normal subject in the upper panel (color scale range 0–2.75  $\mu\text{mole/g/min}$ ) and for the patient with inferior myocardial infarction, shown in Figure 1, in the lower panel (range 0–1.63  $\mu\text{mole/g/min}$ ).

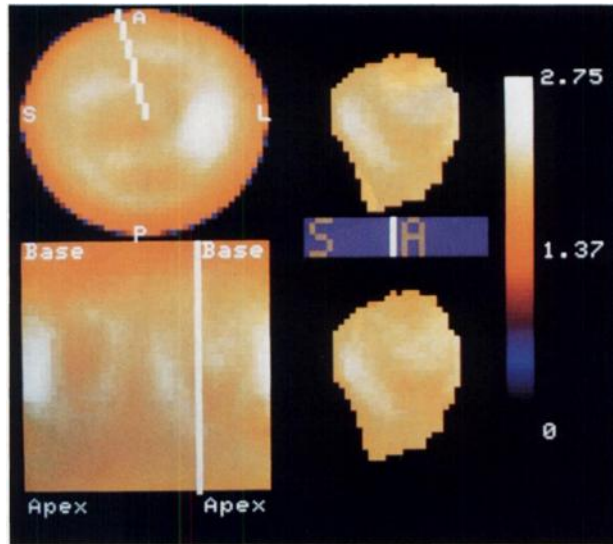


**FIGURE 3**  
The three-dimensional images of  $\dot{M}\text{V}\text{O}_2$  are shown for the normal subject shown in Figure 2. The upper left image is the polar, bull's-eye display while the lower left image is a cylindrical view. The two images on the right are the surface displays with the heart oriented vertically. The white lines in the polar and cylindrical displays rotate in synchrony with the rotation of the surface displays. The bar represents  $\dot{M}\text{V}\text{O}_2$  in units of  $\mu\text{mole/g/min}$ .

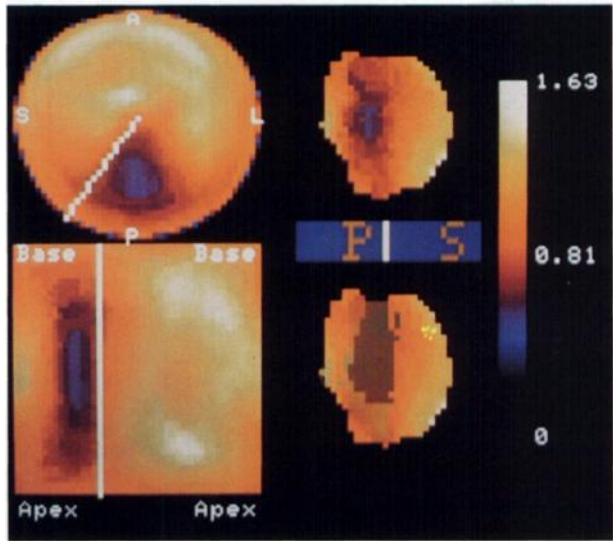


**FIGURE 4**  
The three-dimensional images are shown for the patient with inferior wall infarction presented in Figures 1 and 2.

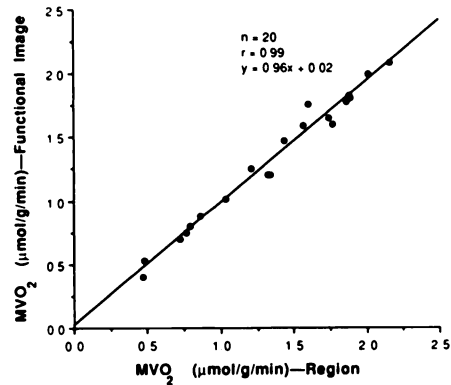


**FIGURE 5**  
Values of  $\dot{M}\text{V}\text{O}_2$  in 20 regions with area  $\sim 1 \text{ cm}^3$  are shown for the previously-validated region method and for the new functional images.

blood pool. The excellent correlation between the functional images and the method employing large regions, shown in Figure 5, coupled with the previously reported observation that the blood pool clears very rapidly (3–5), indicates that such potential contamination by the filtering procedure is unimportant.

### Clinical Implications

The three-dimensional display of functional images provides a quantitatively accurate visual presentation of myocardial oxygen consumption of the human heart that should permit enhanced appreciation of cardiac PET data. The technique is applicable to other dynamic PET studies provided the tracer used and the mathematical model employed are physiologically valid.

### ACKNOWLEDGMENTS

This work was supported in part by National Heart, Lung, and Blood Institute grant HL17646, Specialized Center of Research in Ischemic Heart Disease and by grant HL42884.

This work was presented as an abstract at the annual meeting of The Society of Nuclear Medicine in June, 1989.

### REFERENCES

1. Ritchie JL, Williams DL, Harp G, Stratton JL, Caldwell JH. Transaxial tomography with thallium-201 for detecting remote myocardial infarction. *Am J Cardiol* 1982; 50:1236–1241.
2. Brown M, Marshall DR, Sobel BE, Bergmann SR. Delineation of myocardial oxygen utilization with carbon-11-labeled acetate. *Circulation* 1987; 76:687–696.
3. Brown MA, Myears DW, Bergmann SR. Noninvasive assessment of canine myocardial oxidative metabolism with carbon-11-acetate and positron emission tomography. *J Am Coll Cardiol* 1988; 12:1054–1063.
4. Brown MA, Myears DW, Bergmann SR. Validity of estimates of myocardial oxidative metabolism with carbon-11-acetate and positron emission tomography despite altered patterns of substrate utilization. *J Nucl Med* 1989; 30:187–193.
5. Henes CG, Bergmann SR, Walsh MN, Sobel BE, Geltman EM. Assessment of myocardial oxidative metabolic reserve with positron emission tomography and carbon-11-acetate. *J Nucl Med* 1989; 30:1489–1499.
6. Walsh MN, Geltman EM, Brown MA, et al. Noninvasive estimation of regional myocardial oxygen consumption by positron emission tomography with carbon-11-acetate in patients with myocardial infarction. *J Nucl Med* 1989; 30:1798–1808.
7. Pike VW, Eakins NM, Allan RM, Selwyn AP. Preparation of [ $^{11}\text{C}$ ]acetate—an agent for the study of myocardial metabolism by positron emission tomography. *J Appl Radiat Isot* 1982; 33:505–512.
8. Buxton DB, Schwaiger M, Nguyen A, Phelps ME, Schelbert HR. Radiolabeled acetate as a tracer of myocardial tricarboxylic acid cycle flux. *Circ Res* 1988; 63:628–634.
9. Armbrecht JJ, Buxton DB, Brunken RC, Phelps ME, Schelbert HR. Regional myocardial oxygen consumption determined noninvasively in humans with [ $^{11}\text{C}$ ]acetate and dynamic positron tomography. *Circulation* 1989; 80:863–872.
10. Armbrecht JJ, Buxton DB, Schelbert HR. Validation of [ $^{11}\text{C}$ ]acetate as a tracer for noninvasive assessment of oxidative metabolism with positron emission tomography in normal, ischemic, postischemic, and hyperemic canine myocardium. *Circulation* 1990; 81:1594–1605.
11. Miller TR, Wallis JW, Bergmann SR. Three-dimensional characterization of cardiac metabolism and function by PET [Abstract] *J Nucl Med* 1989; 30:808.
12. Miller TR, Starren JB, Grothe RA. Three-dimensional display of positron emission tomography of the heart. *J Nucl Med* 1988; 29:530–537.
13. Castleman KR. *Digital image processing*. Englewood Cliffs, NJ: Prentice-Hall, Inc.; 1979:414.
14. Miller TR, Sampathkumaran KS, King MA. Rapid digital filtering. *J Nucl Med* 1983; 24:625–628.